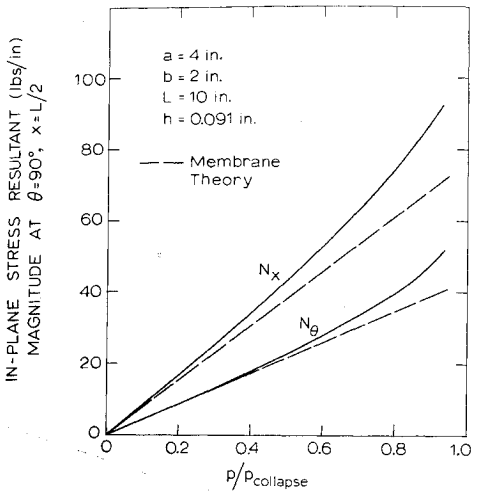


**Fig. 6 Effects of nonlinearities on in-plane stress resultants.**

The same imperfection sensitivity illustrated in Fig. 4 was also observed for a shell with $h = 0.029$ in. This should explain those discrepancies between theory and experiment noted in Refs. 1 and 2 for shells with thicknesses of 0.029 in. or less.

Due to the marked sensitivity of the collapse pressure to a slight change in shape for this type of shell, the effect of the $b/a$ ratio on the collapse pressure was investigated. Table 2 shows the collapse pressures for a shell with $h = 0.049$ in., $L = 10$ in., and a constant circumference c) of 19.38 in. The results are plotted in Fig. 5. Note that for $a = 4.05$ in. and $b = 1.95$ in., the collapse pressure is higher than that for the imperfect shell of Fig. 4. This is due to the fact that the results of Fig. 5 are based on an initially straight sided cylinder while the sides of the imperfect shell of Fig. 4 are initially curved.

One reason for the difference between bifurcation buckling and nonlinear collapse results can be explained with the aid of Fig. 6 which compares the in-plane stress resultants at the minor axis apex of linear membrane theory with those computed by STAGS for a cylinder with a thickness of 0.091 in. The plot for a cylinder with a thickness of 0.029 in. is very similar except that there is very little difference in the $N_\theta$ values. The axial stress resultant ($N_x$) computed by STAGS becomes significantly greater than the membrane $N_x$ for both cases as the pressure approaches the collapse pressure. However, for the hoop stress resultants ($N_\theta$) the difference near collapse is only about 7% for $h = 0.029$ in. while it is about 26% for $h = 0.091$ in. This clearly indicates that the thicker shell allows a flattening effect at $\theta = \pi/2$ to occur due to its greater bending stiffness, whereas the thinner shell begins to collapse at the first sign of flattening.

A bifurcation type analysis cannot account for the flattening effect noticed for thicker shells; hence bifurcation buckling pressures will always be higher than the nonlinear collapse pressure.

It can be concluded that nonlinear effects are very important for this type of shell and that a linear bifurcation type of analysis should be used with caution for shells with a radius of curvature to thickness ratio ($r/h$) less than 270 ($h = 0.029$ in., $a = 4$ in., $b = 2$ in.). It would appear that for $r/h > 270$, a bifurcation buckling should give good results and for $r/h < 270$ ($h = 0.049$ in., $a = 4$ in., $b = 2$ in.) a nonlinear analysis should be used. In all cases, however, any imperfections should be accounted for.

### References

[1] Yao, J. C. and Jenkins, W. C., "Buckling of Elliptic Cylinders Under Normal Pressure," *AIAA Journal*, Vol. 8, No. 1, Jan. 1970, pp. 22–27.

[2] Bushnell, D., "Stress, Buckling and Vibration of Prismatic Shells," *AIAA Journal*, Vol. 9, No. 10, Oct. 1971, pp. 2004–2013.

[3] Almroth, B. O., Brogan, F. A., and Marlowe, M. B., "Collapse Analysis for Elliptic Cones," *AIAA Journal*, Vol. 9, No. 1, Jan. 1971, pp. 32–36.

[4] Brogan, F. and Almroth, B. O., "Buckling of Cylinders with Cutouts," *AIAA Journal*, Vol. 8, No. 2, Feb. 1970, pp. 236–240.

[5] Koiter, W. T., "General Equations of Elastic Stability for Thin Shells," *Proceedings—Symposium on the Theory of Shells to Honor Lloyd Hamilton Donnell*, Univ. of Houston, Houston, Texas, 1967, pp. 187–227.

# Development of a Sonic Boom Simulator with Detonable Gases

R. T. Strugielski,* L. E. Fugelso,† and W. J. Byrne‡
*General American Research Division, Niles, Ill.*

### Introduction

THE advent of supersonic aircraft to the field of commercial transportation is accompanied by several significant problems. Paramount among these problems is the generation of a distinctive pressure pattern known as sonic boom and its effects. At points far away from the aircraft the pressure pattern takes the shape of a classical $N$-wave.

In order to evaluate the effect of sonic booms on structures and human beings the desirability of developing a reliable, low-cost experimental technique capable of reproducing full-scale booms is apparent. One such technique is the generation of weak air-shock waves by the detonation of detonable-gas mixtures contained in thin mylar balloons. In order to develop an $N$-wave generating capability with balloons filled with detonable gases the balloon geometries which produce $N$-wave-forms must be determined. Once they are determined, an efficient experimental procedure must be devised such that field deployment is accomplished with ease and acceptable cost. These two aspects, namely, determining the family of $N$-wave generating balloons and detonation of said balloons, gave impetus to the reported program.

### Conceptual Background

The use of distributed explosives to generate shock waves in air to simulate the pressure profiles expected in a sonic booms

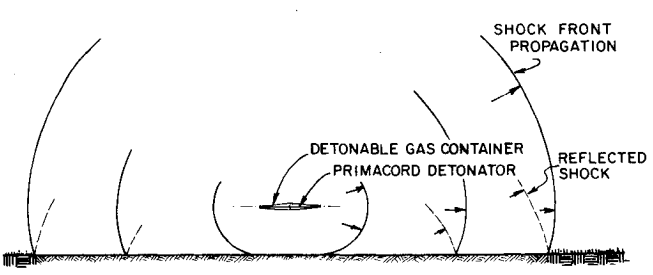


**Fig. 1 Conceptual detonable gas simulation.**

Presented as Paper 71-186 at the AIAA 9th Aerospace Sciences Meeting, New York, January 25–27, 1971; submitted February 2, 1971; revision received June 25, 1971. This study was sponsored by the Federal Aviation Administration and administered by NASA under Contract No. NAS1-9252; Index Categories: Supersonic and Hypersonic Flow, Shock Waves and Detonations.

* R. T. Strugielski, Research Engineer, Applied Mechanics Group.

† L. E. Fugelso, Senior Engineer, Applied Mechanics Group.

‡ W. J. Byrne, Group Leader, Applied Mechanics Group. Associate Member AIAA.

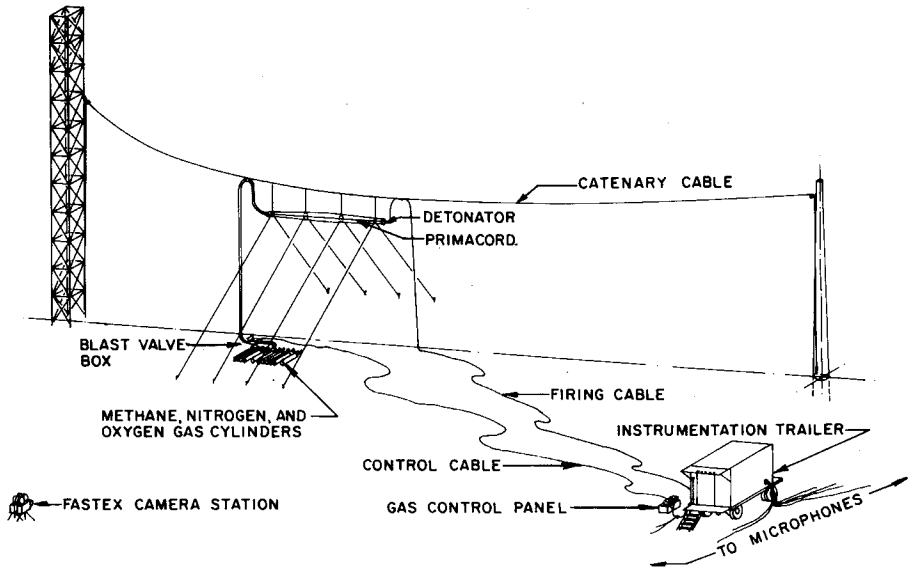


**Fig. 2 Test site.**

was demonstrated by Hawkins and Hicks.[1] A sequence of programs by Balcerzak and Johnson[2] has demonstrated that detonable gas explosions can be used to generate air blast waves which simulate solid explosive detonations. Both demonstrations suggested that if a detonable gas mixture could be dispersed in a long, approximately cylindrical envelope, the ensuing detonation of this mixture would drive an air shock which would have features similar to those of a sonic boom. Variation of the shape of the pressure profile could be made by varying the diameter of the balloon along its length.

The concept is illustrated in Fig. 1. Here a thin plastic envelope in the shape of two truncated cones joined at their bases contains a detonable gas mixture. Primacord is placed along the axis of the envelope. Ignition of the Primacord will cause the gas mixture to detonate, thus producing a time-dependent pressure field in the external atmosphere. The characteristics of the pressure profiles are directly related to the geometrical properties of the plastic envelope and the initial conditions of the detonable gas mixture.

### Experimental Technique

The experimental portions of the program were organized in four broad phases. Individual phases obtained the following information: 1) quantitative and qualitative aspects of pressure regimes due to detonation of the gas mixtures, 2) effects of detonation initiation; 3) effects of balloon shape; and 4) $N$-wave generation.

Figure 2 depicts the test site employed during the program. Suspension of a balloon envelope was accomplished by attaching the balloon to the catenary cable with nylon cords. Position stabilization of the balloon was provided by nylon cord tethering lines attached to the balloons and ground stakes. The gas loading system consisted of an array of gas cylinders with associated flow control valves and pipes located near the balloon envelope. Remote control operation of the gas loading system was provided. Pressures were recorded by six high-performance microphones, which had a flat response up to 8 kHz in the overpressure range measured (1 to 60 psf maximum). The array of microphones was located to the right of the pole illustrated in Fig. 2. Photographic coverage was provided by two Fastex motion picture cameras.

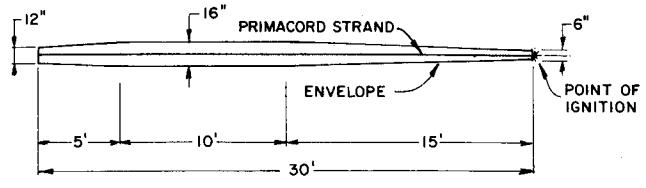


**Fig. 3 Balloon configuration to obtain $N$ wave.**

### Results

The results obtained from the first two phases of the program indicated the following specimen ignition method as optimum. The specimen, when filled with the detonable gas mixture, is suspended from a cable and tethered in a horizontal position 20 ft above the ground. The gas mixture, consisting of methane and oxygen in the molar ratio of one to two, is detonated by a Primacord strand which lies along the cylindrical axis of the balloon specimen. The Primacord, necessary for stabilization of the resulting pressure signal, is ignited by a conventional EB106 detonator at the end of the specimen nearest to the microphone array such that the ensuing Primacord detonation propagates away from the microphone array.

Synthesis of the pressure profile data obtained during the third phase resulted in the fabrication of the balloon illustrated in Fig. 3. Detonation of this balloon shape during the fourth phase produced the downrange pressure profiles illustrated in Fig. 4. The profiles are of the required $N$-shape and examination of the progressively further downrange records indicates progressive signal maturing.

### Conclusions

A pressure profile in the form of an $N$-wave can be generated by the detonation of a shaped, slender gas-filled balloon. A family of such balloons exists which can produce $N$-wave profiles of any desired duration and peak overpressure. The pressure profiles which have been experimentally generated in the described program simulate the pressure signals charac-

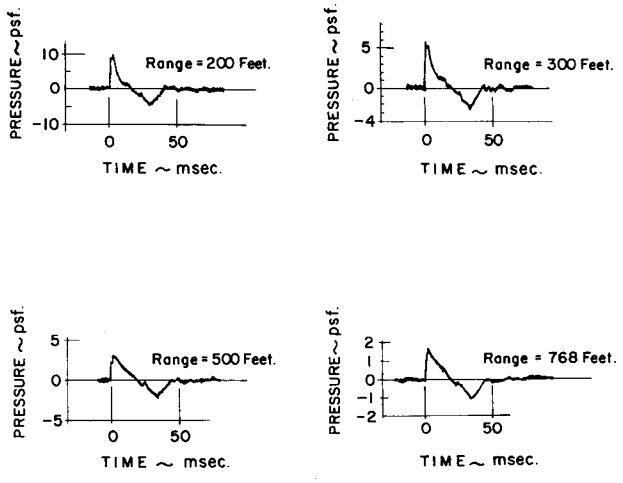


**Fig. 4 Pressure time histories at various ranges.**

terizing sonic booms. Signal durations of up to 75 msec were recorded at distances less than 800 ft from the point of balloon detonation. Peak overpressures in the range 3–15 psf were obtained.

The detonations of gas-filled, slender, shaped balloons of the particular geometry tested in this project yield an $N$-wave at moderate ranges from the source. These balloon detonations could be used directly as pressure signal inputs to a number of sonic boom effect studies. Response studies of structures such as existing buildings and full-scale building components, for example, an exterior wall specimen containing windows and window casements, can be readily and inexpensively tested compared to overflight testing. Since the balloons can be fabricated to any desired size scale, model studies can also be performed. Certain physiological testing might also be considered as this technique generates a signal which does not have much high frequency noise superposed on the signal, a characteristic similar to sonic booms not exhibited by solid explosive simulation.

### References

[1] Hawkins, S. J. and Hicks, J. A., "Sonic Bang Simulation by a New Explosives Technique," *Nature*, Vol. 211, No. 5055, 1966, pp. 1244–1245.

[2] Balcerzak, M. J. and Johnson, M. R., "Use of Detonable Gas Explosions for Blast and Shock Studies," *The Shock and Vibration Bulletin*, Bulletin 37, Pt. 4, Jan. 1968, pp. 199–211.

# Downwash-Velocity Potential Method for Lifting Surfaces

JOHN KENNETH HAVILAND*

*University of Virginia, Charlottesville, Va.*

### Introduction

THIS Note presents some preliminary calculations of subsonic forces on rectangular wings, using the downwash-velocity potential relationship. Generally, the downwash-pressure method has been most widely used, as for example by Watkins[1] and Albano and Rodden.[2] However, Jones,[3] Stark,[4] and Houbolt[5] have used the velocity potential in their methods. Only the steady-state case is considered here.

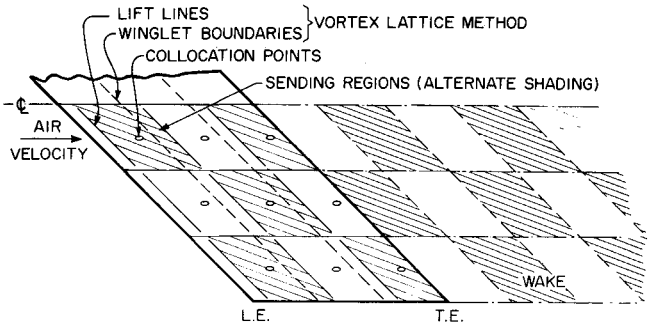


**Fig. 1 Typical wing planform showing equivalent vortex-lattice array.**

Received May 3, 1971; revision received June 10, 1971. This work was carried out for the Vought Aeronautics Company, a division of LTV Aerospace Corporation. Computing time was provided by United Computing Systems Inc.

* Professor of Aerospace Engineering, Department of Aerospace Engineering and Engineering Physics. Associate Fellow AIAA.

**Table 1 Comparison with vortex lattice method**

| | Vortex lattice | These results |
|---|---|---|
| Aspect ratio 2 | $C_{L\alpha} = 3.10902$ | 3.10899 |
| | $C_{M\alpha} = -1.26869$ | −1.26828 |
| Aspect ratio 1 | $C_{L\alpha} = 1.75507$ | 1.75508 |
| | $C_{M\alpha} = -0.53027$ | −0.53027 |

### Derivation

Representing an airfoil by a flat surface parallel to the $x,y$ plane, with a given normal velocity component $w$, the unknown velocity potential jump $\Delta\phi$ is given by the integral equation:

$$w(x,y) = \iint \Delta\phi(\xi,\eta)\partial^2/\partial z^2\{1/4\pi R\}d\xi d\eta \quad (1)$$

where integration is over the wing and wake, with

$$R^2 = (x-\xi)^2 + \alpha^2(y-\eta)^2 + \alpha^2(z-\zeta)^2$$

and $\alpha^2 = 1 - M^2$ ($M$ = Mach number).

Selecting a set of collocation points and denoting "receiving" points by $k$, "sending" points by $l$, the assumption of uniform velocity potential over a sending area region near $l$ leads to the following expression for the downwash at $k$:

$$w_k = \Sigma(l'')\Delta\phi_{l''}k_\phi(k,l'') + \Sigma(l')\Sigma(l^*) \times \exp\{i\omega(x_{l'} - x_{l^*})/V\}\Delta\phi_{l'}k_\phi(k,l^*) = \Sigma(l)A_{k,l}\Delta\phi_l \quad (2)$$

where $l'$ represents a point on the trailing edge, and $l''$ one of the remaining collocation points, while $l^*$ is a point in the wake that is not one of the collocation points. $A_{k,l}$ is the aerodynamic matrix and $k_\phi$ is the airforce influence coefficient, given by

$$k_\phi(k,l) = \iint_{\text{region } l}[\alpha^2/4\pi R^3(k)]d\xi d\eta \quad (3)$$

where $R(k)$ is $R$ evaluated at the point $k$, with coordinates $(x_k,y_k)$. Summation over $l^*$ in Eq. (2) is limited to a finite distance into the wake. An alternate form of Eq. (2) replaces the wake integration by lifting lines along the trailing edge.

For rectangular sending regions having dimensions $L_X$ by $L_Y$, with the point $l$ (coordinates $\xi_l,\eta_l$) at their centers, Eq. (3) can be integrated exactly to give

$$k_\phi(k,l) = F(\xi_l + \tfrac{1}{2}L_X,\eta_l + \tfrac{1}{2}L_Y) - F(\xi_l + \tfrac{1}{2}L_X,\eta_l - \tfrac{1}{2}L_Y) - F(\xi_l - \tfrac{1}{2}L_X,\eta_l + \tfrac{1}{2}L_Y) + F(\xi_l - \tfrac{1}{2}L_X,\eta_l - \tfrac{1}{2}L_Y) \quad (4)$$

where $F(X,Y) = \{(x_k - X)^2 + \alpha^2(y_k - Y)^2\}^{1/2}/4\pi(x_k - X)(y_k - Y)$

Given that the local normal velocity equals the local angle of attack multiplied by the velocity, the velocity potentials in Eq. (2) can be solved by simultaneous equations. From these section lifts and moments can be calculated.

### Preliminary Calculations

These were made on rectangular planforms at uniform angle of attack. In order to get direct verification of the method, the rectangular sending regions were oriented in such a way

**Table 2 Effect of wake length[a]**

| Wake, chord lengths | $C_{L\alpha}$ | $C_{M\alpha}$ |
|---|---|---|
| 1 | 2.6263 | −1.0992 |
| 5 | 2.8390 | −1.1886 |
| 10 | 2.8507 | −1.1935 |
| 50 | 2.8547 | −1.1952 |
| 100 | 2.8548 | −1.1952 |
| 500 | 2.8549 | −1.1953 |

[a] Note convergence to within 1% in five chord lengths.